DE GRUYTER Z. Phys. Chem. 2025; 239(9): 1387–1410

Bernhard Pichler* and Wolfgang Kautek*

Surface investigations of bronze and brass statuary monuments in open-air exposure

https://doi.org/10.1515/zpch-2024-0952
Received July 30, 2024; accepted October 21, 2024; published online April 14, 2025

Abstract: The study of patinas plays an important role in the field of cultural heritage. This review reports systematic investigations of European institutional co-operations. A stable patina relies on a certain atmospheric content of sulphur dioxide from industrial immissions. Since these are decreasing recently, patina phases change to aesthetically unsightly appearances. Analytical case studies are presented of selected bronze monuments and one bronze sculpture in Europe of the period from 1807 until 1934. These were the emperor Joseph II. Memorial (Vienna, Austria), the Maria Theresia Memorial (Vienna, Austria), the Gustav II Adolf Memorial (Gothenburg, Sweden), and the Marquês de Pombal Memorial (Lisbon, Portugal), as well as one Quadriga ensemble on the Austrian Parliament (Vienna, Austria). X-ray diffractometry (XRD), atomic absorption spectral analysis (AAS), scanning electron microscopy (SEM), energy dispersive X-ray microanalysis (EDX), and optical microscopy provided insights into deterioration processes in urban and marine climates. On the basis of these findings suggestions are put forward for innovative conservation interventions on bronze and brass statuary monuments in open-air exposure including laser cleaning technologies which allow the selective removal of encrustations from original patinas.

Keywords: patina; copper; bronze; surface analyses; conservation

1 Introduction

The history of patina can be traced back to its longevity, corrosion resistance and prestigious appearance.[1–3] Corrosion of materials, which are exposed to the atmosphere, is a dynamical process of adaption to varying environments. A patina contains a number of compounds that together create the overall appearance. These include corrosion products and deposited material such as aerosol particles.

***Corresponding authors: Bernhard Pichler**, Institute of Art and Technology, University of Applied Arts Vienna, Salzgries 14, 1010 Vienna, Austria, E-mail: bernhard.pichler@uni-ak.ac.at; and **Wolfgang Kautek**, Department of Physical Chemistry, University of Vienna, Währinger Strasse 42, 1090 Vienna, Austria, E-mail: wolfgang.kautek@univie.ac.at. https://orcid.org/0000-0003-2772-2049 (W. Kautek)

Outdoor copper or bronze objects exhibit patina layers with several components[4–14] such as cuprite, Cu_2O, the hydroxy sulphates brochantite, $Cu_4(OH)_6SO_4$, antlerite, $Cu_3(OH)_4SO_4$, and the hydroxy chloride dimorphs atacamite and paratacamite (=clinoatacamite) $Cu_2(OH)_3Cl$. Posnjakite, $Cu_4(OH)_6SO_4{\cdot}H_2O$, is a common corrosion product after more than ten years exposure.[9,10,15–17] Also strandbergite, $Cu_{2.5}(OH)_3SO_4{\cdot}2H_2O$, and chalcanthite, $CuSO_4{\cdot}5H_2O$, have been observed in outdoor patinas. Cuprite and brochantite dominate on rain-washed light green areas, while copper hydroxy chloride, $Cu_2(OH)_3Cl$, and antlerite, $Cu_3(OH)_4SO_4$, occur in dark rain-sheltered areas.[10] An inner layer of cuprite (Cu_2O) and an outer layer mainly of brochantite ($Cu_4SO_4(OH)_6$) is common.[3,18,19]

The brochantite formation reaction is[20]

$$4Cu^{2+} + SO_4^{2-} + 6H_2O \rightarrow Cu_4\,(OH)_6SO_4 + 6H^+ \tag{1}$$

and for the antlerite formation applies

$$3Cu + SO_4^{2-} + 4H_2O \rightarrow Cu_3\,(OH)_4SO_4 + 4H^+ \tag{2}$$

Atacamite can be formed in chloride-containing environments:[10,21]:

$$4CuCl + O_2 + 4H_2O \rightarrow 2Cu_2\,(OH)_3Cl + 2HCl. \tag{3}$$

Brochantite is stable between 3.5 and 6.5 pH, while antlerite, $Cu_3(OH)_4SO_4$, occurs only in the acidic range between 2.8 and 3.5 pH.[6,11,22] Chalcanthite, $CuSO_4{\cdot}5H_2O$, on an artefact points to the fact that the pH was even <2.8. This shows that bronchantite is the only stable patina phase in a neutral and mildly acidic, humid environment containing SO_2. That means that a patina formed in the inner terrain industrial environment of Central Europe consists mainly of bronchantite.

Therefore, green patina phases were synthesised, particularly the most stable type, brochantite, $Cu_4(OH)_6SO_4$,[1,23–28] The synthesis by a solution-chemical technology of artificial brochantite patination layers was e.g. applied 2004 at the tambour sheeting (approx. 400 m²) of the Otto Wagner Church in Steinhof in Vienna (Figure 1).[24,26] Scanning electron microscopy (SEM) images of the surface textures of the typical reddish coloured cuprite and the greenish brochantite are shown in Figure 2.

The build-up of a black patina and the presence and a synergistic interaction of the oxidising agents SO_2 + NO_2 and SO_2 + O_3 leads to a high corrosion rate.[30–32] Corrosion of bronzes is affected by alloying elements. For instance, it is reduced upon increasing the tin content[33–36] and is changed on quaternary bronzes (Cu–Zn–Sn–Pb).[37]

In order to address immissions in a systematic way, reference can be made to the international standard ISO 9223,[38] which classifies atmospheres and the deposition rate of the most common pollutants: sulphur dioxide and atmospheric salinity. SO_2

(a) (b)

Figure 1: Artificial brochantite patination for the tambour sheeting of the Otto Wagner Church in Steinhof, Vienna, 2004. (a) Bath with submersed copper sheet, (b) tambour with new sheeting.

emissions in Europe increased steadily until about 1980, and decreased afterwards until now.[29,39–42] Specific Viennese SO_2 immission results are depicted in Figure 3. The main reasons for this decline are a reduced sulphur content in mineral oil products, the installation of desulphurisation units and the shutdown of coal-fired power stations partially due to environmental legislation. In Austria, in particular, SO_2 emissions have been reduced by 59.4 % since 2005 and by 85.7 % since 1990.[43]

The degree of atmospheric corrosion of cultural artefacts and a risk assessment can be carried out using experimentally deduced so-called dose-response functions for a variety of materials.[42] In fact, the average annual mass losses show a decrease in the last decades, especially after about 2000, as air pollution decreased.[44,45]

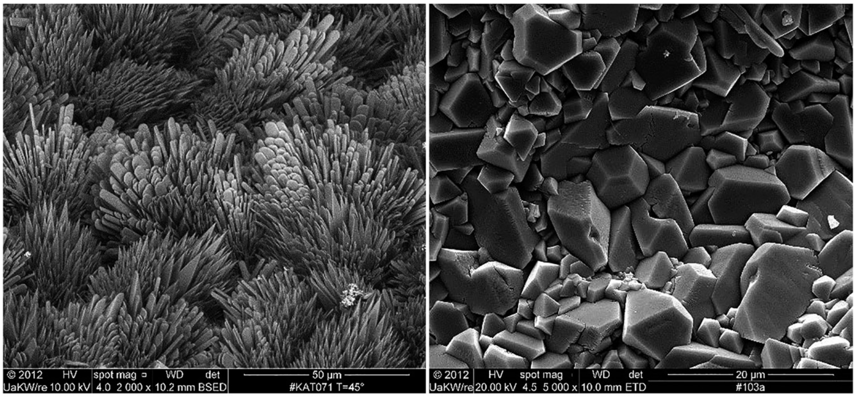

(a) (b)

Figure 2: SEM micrographs of artificial patinas according to Pichler method.[24] (a) Artificial brochantite, $Cu_4[(OH)_6SO_4]$, (b) artificial cuprite, Cu_2O.

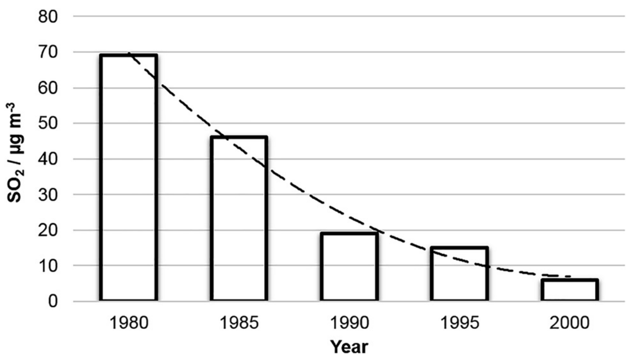

Figure 3: Decline in annual mean SO_2 air concentration in Vienna, 1980–2000.[29] Dashed line indicates trend over two decades.

It has been recognised that the ratio of cuprite to copper salts has generally increased on copper and bronze exposed to the outdoors in recent decades. This is a result of lower SO_2 concentrations and decreased acidity of precipitation.[29,39–42] The expectation that copper and bronze will "naturally" turn green, an aesthetic ideal caused by environmental pollution that developed in the early industrial era, can therefore no longer be achieved today. As a result, streaky and blotchy appearances of old bronze sculptures are more widespread. Such corrosion phenomena have been investigated in the present case study.

As a rule a broad bandwidth of physicochemical methods is used to get an insight into deterioration phenomena on outdoor bronze monuments. This is also responsible for further research findings in the research of copper and copper alloys corrosion.

This paper has been arranged as a review article. The results of extended international co-operations, mostly under the umbrella of the EUREKA Project EU 316 EUROCARE COPAL, have been partially reported in difficult to access grey literature. Therefore, this work offers a review of surface investigations of bronze and brass statuary monuments in open-air exposure, which have been compiled over many years.

2 Methodology

A large repertoire of analytical methods is available for the investigation of corrosion phenomena on outdoor bronzes.[46] Common techniques are optical microscopy (metallography),[3,47,48] X-ray diffractometry (XRD), scanning electron microscopy (SEM), energy dispersive X-ray microanalysis (EDX), and colorimetry.[14,49]

The phase analysis of the patina samples taken with a scalpel was carried out using X-ray diffractometry (XRD; Philips X'pert MPD, CuKα tube, 40 kV, 40 mA). The evaluation of the patina powder samples using XRD was accompanied by light microscopic and electron microscopic SEM-EDX examinations.

Atomic absorption spectral analysis (AAS) was used to determine the composition of the metal samples (drill chips; ~10 mg). These drill chips were cleaned and dissolved in a mixture of HNO_3 and HCl. This solution was analysed in an AAS spectrometer (Perkin Elmer AAS Modell 1100 B).

Additional alloy analyses were carried out using scanning electron microscopy (SEM; Philips XL30 ESEM, 20 kV acceleration voltage) and energy dispersive X-ray microanalysis (EDX; Oxford Instruments, Link ISIS 300) for element-specific distribution images of polished cross-sections.

Metallographic examination methods were used for characterisation of the alloy bulk samples with regard to casting details and patina stratigraphy.[48] The samples were embedded in a cold-hardening synthetic resin, were then wet-ground with SiC paper (grit size 4,000), and polished with diamond pastes (grit sizes 3, 1 and 0.25 µm). For SEM, these specimen were vapour-coated with carbon. A back-scattered detector (BSE) was used.

After completion of the SEM analyses, the polished sections were etched with a copper ammonium chloride solution to develop the metal microstructure for the optical microscopic microstructural examination (Leitz ORTHOPLAN-POL).

3 Analytical case studies

3.1 Alloy analyses

Determining the alloy compositions is a fundamental step in the process of assessing the condition of the object and the strategy of restoration and conservation measures. The objects covered here are made of bronze. The main component is Cu around 90 % (Table 1). The Sn content is in the range 6–10 % with the notable exception of the monument of Emperor Josef II with only approx. 1 %. This particular artefact has a higher Zn content (approx. 6 %) compared to the other objects, which show less than 3 %. The alloys used for the quadriga on the northeast corner of the south wing of the Austrian parliament (comp. Figure 8) is bronze contain copper (ca. 90 %) and tin (ca. 10 %).

The metallographic evaluation sample of the horsetail the Gideon Ernst von Laudon statue of the Maria Theresia Memorial shows a black crust on a partially corroded parent metal. The basic structure is dendritic (Figure 4a). Preferentially one component of the alloy was converted to a green corrosion phase which

Table 1: Alloy compositions of exemplary memorials and ensembles.

	Cu	Sn	Pb	Zn	Fe	Ni	Ag	Sb	As
Peter the Great (1782)	88.63	7.93	0.30	2.62	0.03	0.08	0.03	0.03	0.07
Joseph II (1807)	91.96	1.29	0.42	5.92	0.12	0.08	0.05	0.11	0.08
Gustav II. Adolf (1854)	90.23	6.21	2.11	0.73	0.16	0.08	0.05	0.11	0.32
Quadriga (1885)[a]	89.09	10.18	–	–	–	0.66	–	0.56	0.5
Maria Theresia (1887)	88.62	8.23	0.19	2.59	0.02	0.08	0.05	0.06	0.16
Marquês de Pombal (1934)	92.09	6.52	0.58	0.12	0.02	0.13	0.08	0.10	0.35

AAS analyses of drilling chips. [a]SEM/EDX analysis. In weight %.

phenomenon is discussed below. The lower end of the horsetail of the Emperor Joseph II. Memorial exhibits a microstructure with grains of α-solid solutions (Figure 4b). A metallographic colour etching of a sample from the right horse hock of the Peter the Great Monument also shows a dendritic alloy structure (Figure 4c).

3.2 Emperor Joseph II. Memorial, Vienna

Marcus Aurelius on Capitoline Hill in Rome can be considered the archetype of all post-antique equestrian monuments, which exemplary nature was venerated until the early 19th century and against which artists compared their own creations. It formed the iconographic model for all artists of the Renaissance and all subsequent styles. This is also the case with the Memorial of Emperor Joseph II. on Josefsplatz in Vienna, which was unveiled in 1807 (Figure 5).[50] The specific microenvironment has a tremendous impact on the nature of the corrosion products. The monument shows various corrosion regions in dependence on the irrigation direction and the accessibility of wind convection. Local patina samples were taken with a scalpel. The respective phase analyses by X-ray diffractometry (XRD) are presented in Figure 6. The directly rained zones, such as the upper side of the Emperor's arm, the horse's croup and shoulder, predominantly show the green brochantite, $Cu_4(OH)_6SO_4$, phase. Deposits of dust with a calcite component and layers of gypsum have formed in the concealed areas, in the fold of the coat, in the horse's nostril and in the mane area, but also on the horse's belly. In these areas one finds not only this gypsum formation but also the acidic conversion phase of the original brochantite patina, the antlerite, $Cu_3(OH)_4SO_4$, and with increasing acidity, the chalcanthite, $CuSO_4{\cdot}5H_2O$:[19]

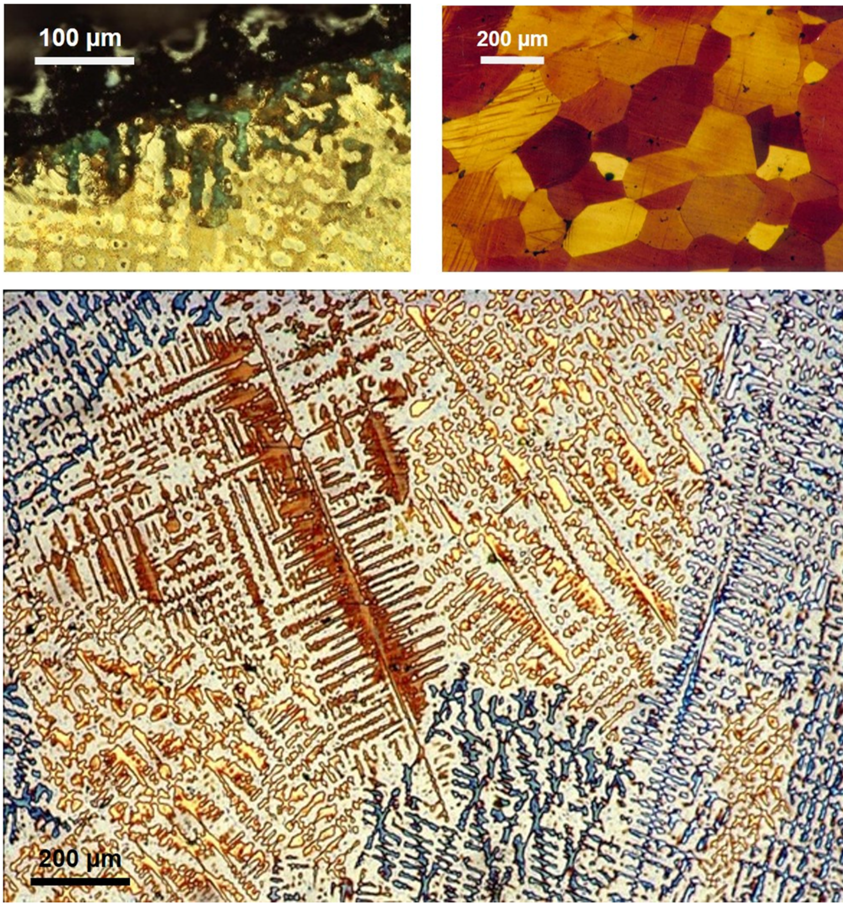

Figure 4: Microstructure analyses. Optical microscopic images of metallographic cross-sections. (a) Gideon Ernst von Laudon statue of the Maria Theresia Memorial, Vienna. Sample from the lower end of the horsetail (#MTH3). Black crust on corroded surface. © University of Applied Arts Vienna. (b) Emperor Joseph II. Memorial, Josefsplatz, Vienna. Lower end of the horsetail (# Josef II/15). Microstructure with grains of α-solid solution. © University of Applied Arts Vienna. (c) Peter the Great Monument on Senate Square, St. Petersburg. Unveiled 1782. Sample from the right horse hock (# LG 12). Dendritic alloy solidification structure. © University of Applied Arts Vienna.

$$3Cu_4(OH)_6SO_4 + H_2SO_4 \rightarrow 4Cu_3(OH)_4SO_4 + 2H_2O \qquad K_{BrAnt} \approx 10^{-18} \qquad (4)$$

and the antlerite is further transformed into chalcanthite:

$$Cu_3(OH)_4SO_4 + 2H_2SO_4 + 5H_2O = 3CuSO_5 \cdot 5H_2O + 4H_2O \qquad K_{AntCh} \approx 10^{-39} \qquad (5)$$

Figure 5: Emperor Joseph II. Memorial, Josefsplatz, Vienna. Unveiled 1807. © University of Applied Arts Vienna.

The equilibrium constant of this reaction is extremely small. That may indicate that the formation of chalcanthite may need a long period. Water layers repeatedly remain there for extended times so that atmospheric SO_2 can increase the concentration of the acid H_2SO_4. Tutton's salt, $(NH_4)_2Cu(SO_4)_2{\cdot}6H_2O$, a rarely occurring mixed basic ammonium sulphate hydrate of copper (II),[51] was detected in sheltered areas, such as in the nostrils, at the lower end of the horse's tail, in the folds of the emperor's robe. It can remain only in hidden regions because it is very soluble and would be washed away in more exposed patina locations.

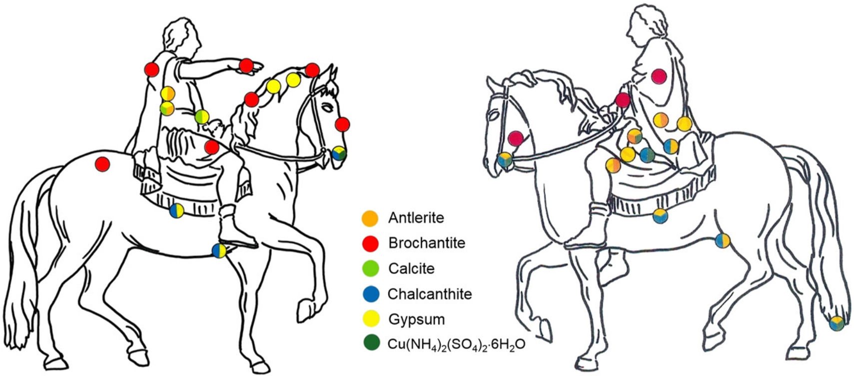

Figure 6: Patina sampling positions and X-ray diffractometry (XRD) results of the Memorial of Emperor Joseph II. Left: Southeast side. Right: Northwest side. © University of Applied Arts Vienna.

3.3 Quadriga on the Austrian Parliament, Vienna

Quadrigas finished in 1885 were restored on the roof of the Austrian parliament in the period 2007–2016.[52] Housings were established for this purpose (Figure 7). XRD data of patina formed on the right wing of a Nike figurine indicates basic copper sulphate, brochantite, as the major corrosion product together with quartz (Figure 8, left). XRD and EDX findings from a sample taken under a removed wheel hub of the left carriage wheel (Figure 8, right) indicate the presence of a chloride bronze patina,

Figure 7: Construction of the housing on the roof of the Austrian parliament for the restoration of one of the Quadrigas. © Parlamentsdirektion, Michael Buchner, Picture ID: 2652377. Date of photograph: 22.08.2007.

Figure 8: Quadriga (1885) on the northeast corner of the south wing of the Austrian parliament before conservation interventions. Left: Right wing of the Nike # Q21a. Right: Left chariot wheel # Q21b. © Atelier Mag. Elisabeth Krebs, Vienna.[52]

the basic copper chloride atakamite, $Cu_2(OH)_3Cl$, a product that usually occurs in the marine environment. The source of the emitter that led to chloride corrosion products has not been resolved. Cl-containing air pollutants, in contrast to NO_2, SO_2, and soot, were not routinely recorded in a dense network of measuring points in Vienna.[29] The basic copper sulphate, brochantite, represents the expected major component. Surface studies have shown that there can be a higher Sn content in the outer area of green areas compared to the outer black regions. It is assumed that in areas that are not regularly irrigated, the originally formed Sn-oxide is covered by deposits and corrosion products, whereas in areas that are constantly exposed to rain, surfaces are cleaned and brochantite or atakamite mainly remain.

3.4 Maria Theresia Memorial, Vienna

The Maria Monument in Vienna (1887) with its four victorious generals on horseback is a work of art from the same period of Ringstrasse construction as the quadriga on the Austrian Parliament building just discussed. An exemplary sample was taken from the lower part of the horse's tail of General Gideon Ernst von Laudon equestrian statue before the restoration in 2013 (Figure 9). The optical image of the surface cross-section shows a black crust on the partially corroded parent metal (Figure 4a). The same region has been analysed by EDX for elemental mapping (Figure 10). The bulk alloy consists mainly of Cu (Figure 10a). In some alloy dendrites, which exhibit intersections with the surface, Cu was depleted in favour of Sn from the base

Figure 9: Gideon Ernst von Laudon of the Maria Theresia Memorial before conservation interventions 2013, Maria Theresia Square, Vienna. © University of Applied Arts Vienna.

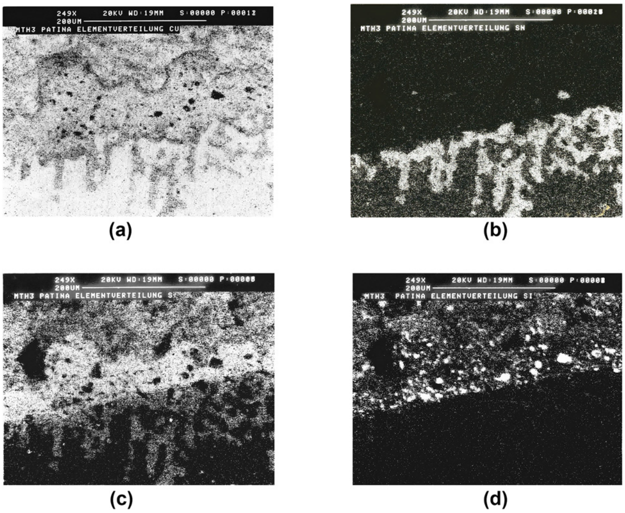

Figure 10: SEM/EDX elemental distribution images of metallographic cross-section (comp. Figure 4a). Gideon Ernst von Laudon statue of the Maria Theresia Memorial, Vienna. Sample of the horsetail (# MTH3). Black crust on corroded surface. (a) Cu, (b) Sn, (c) S, (d) Si. © University of Applied Arts Vienna.

material (Figure 10b) and S coming from the atmosphere (Figure 10c). S and Sn were apparently enriched in these dendrites during the first patina formation period. Silicate dust represented by the Si EDX signal (Figure 10d) has been occluded in the original patina layer, but also above, in the secondary conversion layer which appeared as “black crust”. A distinct interface inside the patina region can be observed by the Cu and S maps. The primary patina, possibly with the major component brochantite, exhibits the highest S content whereas the secondary conversion layer shows more or less a comparable Cu content but a relatively lower S content.

3.5 Gustav II Adolf Memorial, Gothenburg

Gustav II. Adolf, of the Vasa dynasty, was King of Sweden between 1,611 and 1,632 and one of the important figures of Swedish History and of the Thirty Year’s War. His memorial in Gothenburg, Sweden, was unveiled in 1854 (Figure 11). A metallographic cross-section of a sample of the spur on the right boot (Figure 12) reveals a black crust (ca. 30 µm) on top of corrosion layers appearing yellowish and reddish in the cross section image (ca. 60 µm). The reddish component represents cuprite, Cu_2O, which is commonly the first bronze conversion layer.[6,22] The yellow phase may indicate the

Figure 11: Gustav II Adolf Memorial, Gothenburg, Sweden (1854). Aspect from south. © University of Applied Arts Vienna.

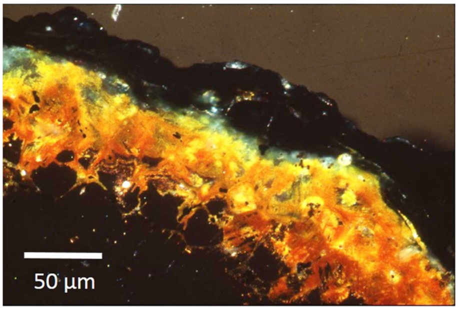

Figure 12: Metallographic cross-section (optical microscopic image). Black crust on corroded surface. Gustav II Adolf Memorial, Gothenburg, Sweden. Sample of the spur on the right boot (# GAGOT 1). © University of Applied Arts Vienna.

presence of Sn-oxide. The thin greenish film underneath the black crust can be correlated with basic Cu sulphates and/or chlorides, such as brochantite, $Cu_4(OH)_6SO_4$, antlerite, $Cu_3(OH)_4SO_4$, and atacamite $Cu_2(OH)_3Cl$.

X-ray diffractometry shows that directly irrigated surfaces (e.g. upper arm, collar, tip of the left boot) contain mainly brochantite and Sn-oxyhydrates accompanied with few Cuprite. Antlerite, which is stable in the more acidic environment, occurs mainly in the cloth pleats (Figure 13). The relative solubility cannot explain the

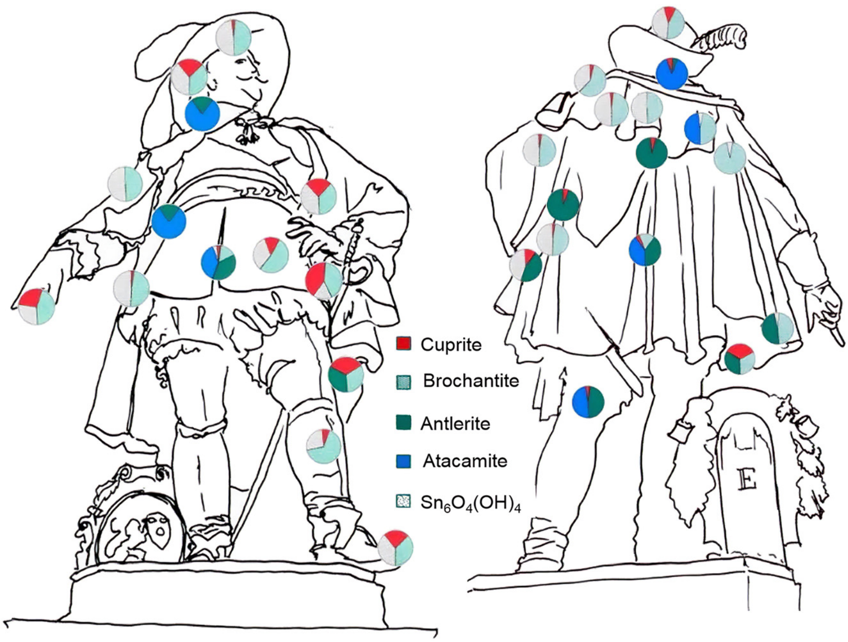

Figure 13: X-ray diffractometry (XRD) results of the Memorial of Gustav II Adolf. Left: South side. Right: North side. Analyses of the relative proportions of the patina components: cuprite, brochantite, antlerite, atacamite, and Sn-oxyhydrates. © University of Applied Arts Vienna.

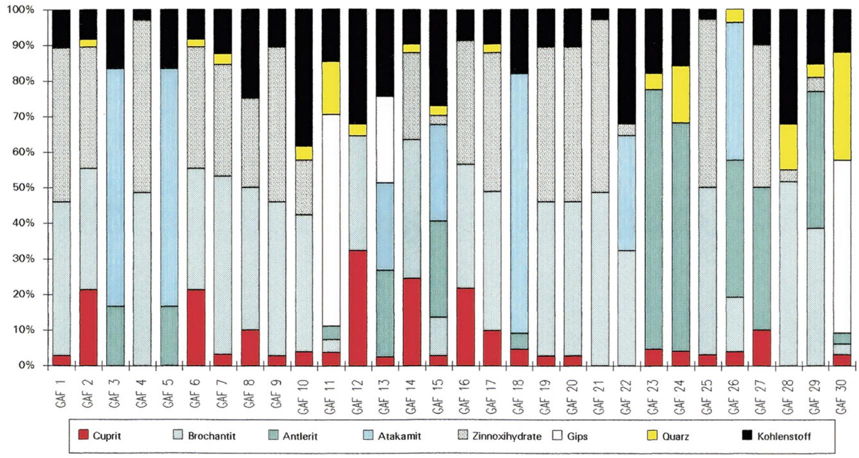

Figure 14: Semiquantitative evaluation of patina mineral components by light microscopy of powder samples.[54] Gustav II Adolf Memorial, Gothenburg, Sweden (1854). South side: positons "GAF" 1–6, 8–12, 14–16. North side: positons "GAF" 7, 13, 17–30. © University of Applied Arts Vienna.

absence of the chloride species, atacamite, in irrigated regions. Therefore, one has to assume that NaCl spray and droplets dry out and result in crystallites which can accumulate in rain-sheltered areas. There, in humid condition, they react with pre-existing brochantite, antlerite, and cuprite.

Patina powder samples were subjected to the semiquantitative evaluation of patina mineral components by light microscopy (Figure 14). Brochantite occurs together with Sn oxyhydrates mainly on irrigated surfaces (position 1, 2, 4, 6, 7, 8, 9, 10, 14, 16, 17, 19, 20, 21, 25, 28, 29). Antlerite and brochantite do not appear together except in a single positions (29). They obviously exclude each other due to their different pH stability. Antlerite, however can be associated with the occurrence of the chloride species, atacamite, in hidden and remote locations where rain cannot arrive directly (positions "GAF" 3, 5, 13, 15, 18, 26), There are also few more or less remote locations where antlerite is only associated with some cuprite, quartz and carbonatious contaminants (positions "GAF" 23, 24). Gypsum accumulated in hidden locations (position "GAF" 11, 13, 30) obviously excluding Sn-oxyhydrates. Interestingly, there are reports[53] that alloying with Sn facilitates the formation of atacamite through redox reactions between intermediate Sn- and Cu-chlorides, based on the strong reducing power of Sn(II)-chlorides. The orientation north versus south side shows no significant influence on the patina character since e.g. the seaside is still at far on Gustaf Adolf's Square.

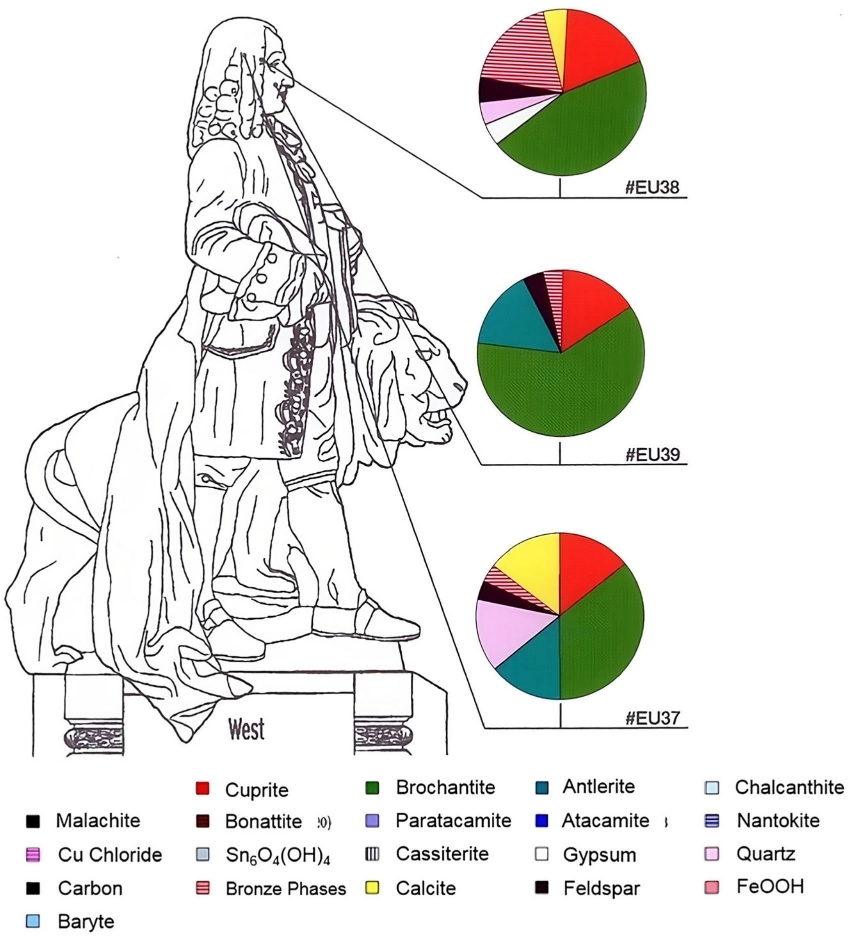

Figure 15: Semiquantitative evaluation of patina mineral components by light microscopy of powder samples.[54] Marquês de Pombal, Lisbon, Portugal, 1934. © University of Applied Arts Vienna.

3.6 Marquês de Pombal Memorial, Lisbon

The monument of the Marquês de Pombal unveiled 1934 is located few kilometres from the Atlantic Ocean, and therefore underwent a typical marine climate. Atomic Absorption Spectroscopy (AAS) of the casting Cu–Sn alloy showed a Sn content of ca. 7 % Sn. Other elements such as Pb, Zn, Ni, Ag, Sb, and As show concentrations of the order of 0.1 %.[24] At exposed and therefore heavily irrigated areas on the head the main patina constituent is brochantite (green) besides cuprite (red) and antlerite (blue-green) (Figure 15). Actually, a total of 49 patina samples were evaluated by the semiquantitative optical microscopy method.[24] In hidden areas chloride containing phases were detected such as atacamite.[55]

4 Test coupons exposure

Standard patinas under various climatic and environmental conditions have started in the 1990s by exposing copper and standard copper alloy (Rg 5 alloy) and artificially patinated copper and copper alloy plates to check the alterations due to environmental local influences. Both inland and marine locations were chosen globally, i.e. in USA, Europe, Asia, and Australia (Table 2). In addition to the standard copper alloy coupons, also alloys according to the compositions of several historical monuments were cast. In this context, the casting technologies applied to produce the monuments were researched.[56–58] A large proportion of these samples showed a dendritic structure. An example is a test coupon with the composition of the Memorial of Emperor Joseph II, Vienna (Figure 16) which was used for outdoor expositions (Table 2).

Protective coatings in the field of outdoor bronze conservation have been broadly applied.[59–61] E.g. organo-silanes[62] and ormoceres[63] were applied also to coupons. Other exposure project are e.g. investigations of the dose-response

Table 2: Locations and starts of the outdoor exposition programme of the University of Applied Arts Vienna, Institute of Art and Technology.

Locations	Starts
Venice, Misericordia Laboratory, Cannaregio	1992
Moscow, Russian Academy of Sciences	1993
Gothenburg, Chalmers University of Technology	1993
St. Petersburg, Aleksandr-Newskij-Monastery	1993
Munich, Bayerisches Landesamt für Denkmalpflege	1993
Vienna, Hermannskogel, MA 22, Umweltschutz	1993
Alfanzina, Laboratorio Nacional de Engenharia Civil (Lisbon)	1995
Copenhagen, Nationalmuseet	1996
Fremantle, Western Australian Museum[a]	1996
Honolulu, St. Andrew's Cathedral, Tower[a]	1997
Stanford, Carl Djerassi SMIP Ranch[a]	1997
New York, The Metropolitan Museum of Art & NYU[a]	1997
Bangkok, Austrian Embassy[a]	1998
Ephesos, Austrian Excavation Center, ÖAI[a]	1999
Mellecey, Chateau de Germolles[a]	2007

[a]Extension of the ISCA/COPAL exposition programme.

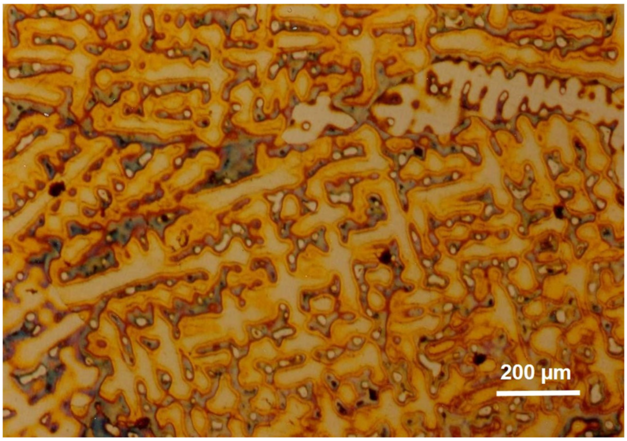

Figure 16: Dendritic structure of the recast alloy with the composition used for the Memorial of Emperor Joseph II, Vienna (comp. Table 1), from Austrian Federal Ministry for Science and Research, final report of the project "EUROCARE-Metallkonservierung", BMWF GZ. 49.599/5–24/88.

functions on dry and wet acid deposition effects[64,65] and of the impact of urban rain on the changes of bare and artificially patinated bronze.[45] The analysis of such exposed coupons includes stereomicroscopy, optical microscopy of surfaces and cross-sections, SEM, EDX, XRD, colorimetry, layer thickness measurements, and also electrochemical evaluations such as electrochemical impedance spectroscopy.

5 Summary

The object conditions described in Section 3 show that for a scientifically based restoration and conservation it is necessary to determine microclimatic data and to define their appropriate recording period. This would necessitate recording, for example, the amount of precipitation, time of wetness, sun hours, the concentration of SO_2, NO_2, O_3, H_2S, COS, HCI, NaCl, $(NH_4)SO_4$ and soot particles in the immediate neighbourhood of the object. In Austria, for example, the concentrations of anthropogenic emissions of NO_x, SO_2, NMVOC (non-methane volatile organic compound), NH_3 and particulate matter (PM2.5), are recorded relatively spatially close together, but not in the immediate vicinity of the artefacts.

The study of the production and characterisation of artificial patinas plays an important role in the field of cultural heritage.[1,3,23–27,36,66] There have been numerous attempts of obtaining a stable artificial brochantite based on the formation from a humid atmosphere containing sulphur dioxide. Due to expected future climate and industrial immission changes[44] this approach may attain a priority.

In the context of innovative techniques to clean outdoor bronze monument and copper-based architectural elements such as roofs, laser cleaning may play an indispensable role. Laser cleaning has become an established conservation intervention technology for a range of artefacts, including stone, ceramics, paintings, and metals in cultural heritage, i.e. copper, iron, silver and gold.[14,67–83] There exists an abundant wealth of experiences with conservation and cleaning techniques for outdoor bronzes which should be considered in modern intervention strategies.[84–90] A minimal intervention to maintain the ageing value would be respecting the patina and the removal of deposits of soot, dust and corrosion products that disfigure the surface.

A careful selection of the laser wavelength, pulse duration and operating conditions is crucial for the laser cleaning outcome. The laser cleaning of metals is often associated with side effects such as discolouration and micro-melting. The use of analytical techniques is crucial to assess the laser cleaning outcomes. When metals are covered with thick coatings or thick corrosion layers, better results can generally be obtained by combining laser cleaning with mechanical cleaning.

The optimal conditions for laser cleaning of bronze patina surfaces would be the case “black over green” areas because a black crust would absorb in most of the used laser wavelengths and would be evaporated. Whereas a green patina phase mainly absorbs radiation in the blue and violet range. Therefore, near wavelengths appear most promising because they show a low interaction with the patina avoiding destructions and modification. Actually, cleaning of patinated copper surfaces with UV and green laser wavelengths results in discoloration and darkening. The visible wavelength 532 nm may lead to damage and roughening. There are however several reports that the IR wavelength allows cleaning without side effect.[14,78,79,91]

Regular maintenance by cleaning and coating with a protective material is a common approach to preserve outdoor patinated bronze. The selection of applicable coatings is limited by the object’s visual unchanged appearance and the reversibility. Common protective materials are waxes, acrylic resins, and corrosion inhibitors.[59–63,92–96] However, waxes have a short lifetime, are not fully reversible, and are prone to dust accumulation. Acrylic coatings from the Paraloid family and Incralac (an acrylic resin solution containing corrosion inhibitors like benzotriazole) are widespread. They require regular maintenance, similar to waxes. Their drawbacks are the shiny appearance, the brittleness of the film, and the difficult removal over time. Transparent coatings show yellowing due to photooxidation. Benzotriazole (BTA) has been applied since the 1960s. Since the long-time effects of such protection coatings can be often very disappointing, their laser removal may play a crucial role in metal conservation praxis.

It is highly recommended that metallic outdoor structures should be regularly inspected by professionals to detect and prevent deteriorations. In the field of sculpture conservation, a maintenance protocol is urgently needed, especially for new works of art.[30,31,97–101]

Regular cleaning and treatment should be carried out by experts. Physico-chemical and analytical application-oriented training programs turned out to bridge the gap between conservators and scientists.

Acknowledgments: Special thanks to Boris Sizov (Moscow), Hans Haiden (University of Applied Arts Vienna) for sampling campaigns, Viktor Chursin (Moscow) for alloy casting of test coupons, Roman Sauer (University of Applied Arts Vienna) for microscopy support, Josef Riederer (Rathgen-Forschungslabor, Staatliche Museen zu Berlin - Preußischer Kulturbesitz, Berlin, Germany) for AAS analyses, Erich Halwax (TU Wien) for XRD analyses, Rute Fontinha and Manuela Salta (National Laboratory for Civil Engineering, LNEC, Lisbon, Portugal) for the sampling campaigns in Lisbon and Alfanzina. Thanks also to the participants of the EUREKA Project EU 316 EUROCARE COPAL as well as to related institutions in USA, Asia and Australia.
Research ethics: Not applicable.
Informed consent: Not applicable.
Author contributions: Both authors have accepted responsibility for the entire content of this manuscript and approved its submission.
Use of Large Language Models, AI and Machine Learning Tools: None declared.
Conflict of interest: The authors declare no conflict of interest.
Research funding: None declared.
Data availability: Not applicable.

References

1. Vanino, L.; Seitter, E. *Die Patina. Ihre natürliche und künstliche Bildung auf Kupfer und dessen Legierungen*; A. Hartleben's Verlag: Wien, Pest, Leipzig, 1903.
2. Scott, D. A. *Metallography and Microstructure of Ancient and Historic Metals*; Getty Conservation Institute in Association with Archetype Books: Marina del Rey, CA, 1991.
3. Scott, D. A. *Copper and Bronze in Art: Corrosion, Colorants, Conservation*; Getty publications: Los Angeles, 2002.
4. Accardo, G. *Marco Aurelio, mostra di cantiere: le indagini in corso sul monumento*; Arti Grafiche Pedanesi: Rome, 1984.
5. Pichler, B. *Symposium on the Conservation of Metal Statuary and Architectural Decoration Exposed in the Open Air*; ICCROM: Paris, 1986; pp 267–290.
6. Graedel, T. E.; Nassau, K.; Franey, J. P. Copper Patinas Formed in the Atmosphere – I. Introduction. *Corros. Sci.* **1987**, *27*, 639–657.
7. Riederer, J. Zur historischen Entwicklung der Kenntnis von Korrosionsprodukten auf kulturgeschichtlichen Objekten aus Kupferlegierungen. *Berl. Beiträge Archäometrie* **1992**, *11*, 93–111.

8. Rubbiola, L.; Fiaus, C.; Pennec, S. *ICOM Committee for Conservation Tenth Triennial Meeting*, Vol. *2*, 1993, pp. 796–802.
9. Selwyn, L. S.; Binnie, N. E.; Poitras, J.; Laver, M. E.; Downham, D. A. Outdoor Bronze Statues: Analysis of Metal and Surface Samples. *Stud. Conserv.* **1996**, *41*, 205–228.
10. Strandberg, H.; Lars-Gunnar, J.; Rosvall, J. Outdoor Bronze Sculptures: a Conservation View on the Examination of the State of Preservation. In *11th Triennial* Meeting; *ICOM Committee for Conservation Triennial Meeting*; James & James: Edinburgh, 1996, pp 894–900.
11. Marabelli, M. *Ancient & Historic Metals: Conservation and Scientific Research*; Scott, David A., Podany, Jerry, Considine, Brian B., Eds., Electronic Edition; The J. Paul Getty Trust: Los Angeles, 2007; pp 1–19.
12. Bogolitsyna, A.; Pichler, B.; Vendl, A.; Mikhailov, A.; Sizov, B. Investigation of the Brass Monument to Minin and Pozharsky, Red Square, Moscow. *Stud. Conserv.* **2009**, *54*, 12–22.
13. Watkinson, D. Preservation of Metallic Cultural Heritage. *Shreir's Corrosion* **2010**, *4*, 3307–3340.
14. Giesriegl, A.; Pacher, U.; Nagy, T.; Pichler, B.; Kautek, W. Laser Diagnostics and Processing of Historical and Artificial Copper Patina. *J. Cult. Herit.* **2023**, *62*, 45–53.
15. Strandberg, H.; Langer, V.; Johansson, L. Structure of $Cu_{2.5}(OH)_3SO_4 \bullet 2H_2O$: A Novel Corrosion Product of Copper. *Acta Chem. Scand.* **1995**, *49*, 5–10.
16. Odnevall, I.; Leygraf, C. Atmospheric Corrosion of Copper in a Rural Atmosphere. *J. Electrochem. Soc.* **1995**, *142*, 3682.
17. Oesch, S.; Heimgartner, P. Environmental Effects on Metallic Materials – Results of an Outdoor Exposure Programme Running in Switzerland. *Mater. Corros.* **1996**, *47*, 425–438.
18. Gettens, R. J. Tin-Oxide Patina of Ancient High-Tin Bronze. *Bulletin Fogg Art Mus.* **1949**, *11*, 16–26.
19. Woods, T. L.; Garrels, R. M. Phase Relations of Some Cupric Hydroxy Minerals. *Econ. Geol.* **1986**, *81*, 1989–2007.
20. Livingston, R. A. Acid Rain Attack on Outdoor Sculpture in Perspective. *Atmos. Environ.* **2016**, *146*, 332–345.
21. Naylor, A. Modern Conservation of Outdoor Bronze Sculpture. In *Monuments and the Millennium*; English Heritage and the United Kingdom Institute for Conservation: London, 1998, pp. 91–96.
22. Graedel, T. E. Copper Patinas Formed in the Atmosphere – II. A Qualitative Assessment of Mechanisms. *Corros. Sci.* **1987**, *27*, 721–740.
23. Hughes, R.; Row, M. *The Colouring Bronzing and Patination of Metals*; Crafts Council: London, 1982.
24. Pichler, B. Analytical Investigations of Outdoor Bronze Monuments: EUREKA Project EU 316 EUROCARE-COPAL. *ICOMOS – Hefte des Deutschen Nationalkomitees* **1998**, *29*, 63–69.
25. Pichler, B.; Vendl, A.; Binder, U. Growth, Description, and Characterization of Natural and Artificial Copper and Bronze Patina with Varying Composition and Thickness. In *Technologies to Protect and Rehabilitate European Cultural Heritage: A Research Area Funded by the EC R & D Programme 'Environment and Climate': Development of a New Non-destructive Method for Analysis of the Atmospheric Corrosion and Corrosion Protection of Copper and Copper Alloys: Protection and Conservation of the European Cultural Heritage: Project ENV4-CT95-0098: (1996–97): Conclusive Report*; Office for Official Publications of the European Communities, 1999; pp 17–95.
26. Mazzeo, R.; Prati, S.; Quaranta, M.; Sciuto, G. An Overview of Analytical Techniques and Methods for the Study and Preservation of Artistic and Archaeological Bronzes. *Mediterr. Archaeol. Archaeom* **2012**, *12*, 261–271.
27. Bureš, R.; Klajmon, M.; Fojt, J.; Rak, P.; Jílková, K.; Stoulil, J. Artificial Patination of Copper and Copper Alloys in Wet Atmosphere with Increased Content of SO_2. *Coatings* **2019**, *9*, 837.
28. Rak, P.; Fink, D.; Bureš, R.; Stoulil, J. Novel Procedure for Brochantite Based Pigment Production and Its Immobilization for Restoration of Historical Copper Objects. *Coatings* **2020**, *10*, 972.

29. Augustyn, R. Municipal Department 22, MA 22, City of Vienna: Vienna, 2001.
30. Strandberg, H.; Johansson, L. G. The Formation of Black Patina on Copper in Humid Air Containing Traces of SO_2. *J. Electrochem. Soc.* **1997**, *144*, 81.
31. Strandberg, H.; Johansson, L.-G.; Lindqvist, O. The Atmospheric Corrosion of Statue Bronzes Exposed to SO_2 and NO_2. *Mater. Corros.* **1997**, *48*, 721–730.
32. Strandberg, H. Reactions of Copper Patina Compounds – I. Influence of Some Air Pollutants. *Atmos. Environ.* **1998**, *32*, 3511–3520.
33. Gianni, L. *Corrosion Behavior of Bronze Alloys Exposed to Urban and Marine Environment: An Innovative Approach to Corrosion Process Understanding and to Graphical Results Presentation*; Ghent University: Belgium, 2011.
34. Gianni, L.; Cavallini, M.; Adriaens, A. Corrosion Behaviour of Bronze in Urban Environments: Influence of Tin Content. *Corros. Eng., Sci. Technol.* **2013**, *48*, 334–339.
35. Chang, T.; Herting, G.; Goidanich, S.; Sánchez Amaya, J. M.; Arenas, M. A.; Le Bozec, N.; Jin, Y.; Leygraf, C.; Odnevall Wallinder, I. The Role of Sn on the Long-term Atmospheric Corrosion of Binary Cu-Sn Bronze Alloys in Architecture. *Corros. Sci.* **2019**, *149*, 54–67.
36. Petiti, C.; Toniolo, L.; Berti, L.; Goidanich, S. Artistic and Laboratory Patinas on Copper and Bronze Surfaces. *Appl. Sci.* **2023**, *13*, 11873.
37. Kwon, H. Corrosion Behaviors of Artificial Chloride Patina for Studying Bronze Sculpture Corrosion in Marine Environments. *Coatings* **2023**, *13*, 1630.
38. Morcillo, M.; Chico, B.; de la Fuente, D.; Simancas, J. Looking Back on Contributions in the Field of Atmospheric Corrosion Offered by the MICAT Ibero-American Testing Network. *Int. J. Corrosion* **2012**, *2012*, 824365.
39. Mylona, S. Sulphur Dioxide Emissions in Europe 1880–1991 and their Effect on Sulphur Concentrations and Depositions. *Tellus B* **1996**, *48*, 662–689.
40. Stöckle, B.; Krätschmer, A. Die atmosphärische Korrosion von Kupfer und Bronze. Ergebnisse aus dem UN/ECE-Bewitterungsprogramm. *ICOMOS – Hefte des Deutschen Nationalkomitees* **1998**, *29*, 26–32.
41. Fitz, S. Entwicklung der Luftgüte in Deutschland. *ICOMOS – Hefte des Deutschen Nationalkomitees* **1998**, *29*, 11–18.
42. Fitz, S. Mapping of Damage and Cost of Cultural Heritage at Different Pollution Scenarios. In *CULT-STRAT; Assessment of Air Pollution Effects on Cultural Heritage – Management Strategies*; Umweltbundesamt Germany: Berlin, 2007; p 49.
43. Anderl, M.; Gangl, M.; Lampert, C.; Mayer, S.; Pazdernik, K.; Perl, D.; Poupa, S.; Purzner, M.; Schieder, W.; Schmidt, G.; Schodl, B.; Stranner, G.; Wieser, M. *Air Emission Trends 1990–2020*; Environment Agency Austria: Vienna, 2022; p 49.
44. Pålsson, N. T.; Johan, T.; Kreislova, K.; Faller, M.; De la Fuente, D.; Yates, T.; Verney-Carron, A.; Vuorio, T. *Trends in Pollution, Corrosion and Soiling 1987–2019*; Rise: Sweden, 2019.
45. Kosec, T.; Leban, M. B.; Ropret, P.; Finšgar, M. The Impact of Urban Rain on the Changes of Bare and Artificially Patinated Bronze During 9-Year Exposure. *Environ. Sci. Pollut. Res.* **2024**, *31*, 31925–31941.
46. Gigante, G. E.; Diana, M. *Metodologie fisiche non distruttive per le indagini sui beni culturali*; Università degli Studi di Roma "La Sapienza": Rome, 2005.
47. Franey, J. P.; Davis, M. E. Metallographic Studies of the Copper Patina Formed in the Atmosphere. *Corros. Sci.* **1987**, *27*, 659–668.
48. Mach, M.; Reinhardt, C.; Snethlage, R. Elementverteilungsbilder von Querschnitten durch Bronze- und Kupferpatina von Objekten im Freien. *Wiener Berichte über Naturwissenschaften in der Kunst* **1987**, *4/5*, 214–219.

49. Gianni, L.; Gigante, G. E.; Cavallini, M.; Adriaens, A. Corrosion of Bronzes by Extended Wetting with Single versus Mixed Acidic Pollutants. *Materials* **2014**, *7*, 3353–3370.
50. Werner, E. *Das Reiterstandbild Josephs II. Am Josefsplatz in Wien*; University of Vienna: Vienna, 2013.
51. Bernardini, G.; Corazza, M.; Olmi, F.; Sabelli, C. The Incredulità di San Tommaso by Verrocchio: A Mineralogical Study of Alteration Patinas. *Sci. Technol. Cult. Herit.* **1992**, 177–189.
52. Pichler, B.; Weber, J. *Naturwissenschaftliche Untersuchungen an Proben einer Quadriga des Parlamentsgebäudes, Wien I im Auftrag der Parlamentsdirektion Wien*; University of Applied: Arts Vienna: Vienna, 2000.
53. Chang, T.; Maltseva, A.; Volovitch, P.; Odnevall Wallinder, I.; Leygraf, C. A Mechanistic Study of Stratified Patina Evolution on Sn-Bronze in Chloride-Rich Atmospheres. *Corros. Sci.* **2020**, *166*, 108477.
54. Sauer, R. *Semiquantitative Evaluation of Patina Mineral Components by Light Microscopy of Powder Samples*; University of Applied Arts: Vienna: Vienna, 1990.
55. Fonseca, I. T. E.; Picciochi, R.; Mendonça, M. H.; Ramos, A. C. The Atmospheric Corrosion of Copper at Two Sites in Portugal: A Comparative Study. *Corros. Sci.* **2004**, *46*, 547–561.
56. Chursin, V. M.; Vendl, A.; Pichler, B. Big Cast Bronze Monuments – Treasures of Castings Technologies. *Литейное Производство (The Foundry)* **1994**, 24–30.
57. Chursin, V.; Vendl, A.; Pichler, B. From the History of Creation of Copper-Base Alloys. *Цветные Металлы (Non-ferrous Metals)* **1995**, 47–51.
58. Chursin, V. The Assessment of the Cast Quality of Monuments on the Basis of the Analysis of the Copper Alloy Casting Properties. *ICOMOS – Hefte des Deutschen Nationalkomitees* **1998**, *29*, 52–55.
59. Smith, R.; Beale, A. *An Evaluation of the Effectiveness of Various Plastic and Wax Coatings in Protecting Outdoor Bronze Sculpture Exposed to Acid Deposition: a Progress Report, Conservation of Metal Statuary and Architectural Decoration in Open-air Exposure, Symposium, Paris, 6-8*. *X*. 1986, 1987, pp. 99–124.
60. Brostoff, L. B. *Coating Strategies for the Protection of Outdoor Bronze Art and Ornamentation*; Universiteit van Amsterdam: Amsterdam, 2003.
61. Molina, M. T.; Cano, E.; Ramírez-Barat, B. Protective Coatings for Metallic Heritage Conservation: A Review. *J. Cult. Heri.* **2023**, *62*, 99–113.
62. Fontinha, R. On the Way to Find Innovative Treatments for the Protection of Outdoor Bronze Monuments. In *Materiais 2019, XIX Congresso da Sociedade Portuguesa de Materiais and X International Symposium on Materials*: Lisbon, 2019
63. Römich, H.; Pilz, M. Materialentwicklung für die Bronzekonservierung. *ICOMOS–Hefte des Deutschen Nationalkomitees* **1998**, *29*, 85–89.
64. Stöckle, B.; Fitz, S.; Mach, M.; Pöhlmann, G.; Snethlage, R. Die atmosphärische Korrosion von Kupfer und Bronze im Rahmen des UN/ECE-Expositionsprogramms. Zwischenbericht nach 4-jähriger Bewitterung. *Mater. Corros.* **1993**, *44*, 48–56.
65. Tidblad, J.; Kucera, V.; Mikhailov, A. A.; Henriksen, J.; Kreislova, K.; Yates, T.; Stöckle, B.; Schreiner, M. UN ECE ICP Materials: Dose-response Functions on dry and Wet Acid Deposition Effects After 8 Years of Exposure. In *Acid rain 2000: Proceedings from the 6th International Conference on Acidic Deposition: Looking Back to the Past and Thinking of the Future Tsukuba, Japan, 10–16 December 2000 Volume III/III Conference Statement Plenary and Keynote Papers*; Satake, K., Ed.; Kluwer Academic Publishers: Dortrecht, 2001; pp 1457–1462.
66. Fitzgerald, K. P.; Nairn, J.; Atrens, A. The Chemistry of Copper Patination. *Corros. Sci.* **1998**, *40*, 2029–2050.
67. Siano, S. Pulitura Laser di Manufati Metallici. In *Monumenti in bronzo all'aperto: esperienze di conservazione a confronto*; Nardini Editore: Florence, 2004; pp 99–106.
68. Degrigny, C.; Tanguy, E.; Le Gall, R.; Zafiropulos, V.; Marakis, G. Laser Cleaning of Tarnished Silver and Copper Threads in Museum Textiles. *J. Cult. Herit.* **2003**, *4*, 152–156.

69. Fotakis, C.; Anglos, D.; Zafiropulos, V.; Georgiou, S.; Tornari, V. *Lasers in the Preservation of Cultural Heritage: Principles and Applications*; CRC Press: Boca Raton, 2006.
70. Fridevaux, M.; Platt, P.; Cooper, M.; Watkins, K. Laser Interaction With Copper, Copper Alloys and Their Corrosion Products Used in Outdoor Sculpture in the United Kingdom. In *Lasers in the Conservation of Artworks, LACONA 7 Proceedings*; Castillejo, M. e. a., Ed.; Taylor & Francis Group: London, 2008; pp 277–284
71. Schreiner, M.; Strlič, M.; Salimbeni, R. *Handbook of the Use of Lasers in Conservation and Conservation Science*; COST Office: Brussels, 2008. http://www.science4heritage.org/COSTG7/booklet/.; Vol.
72. Kautek, W. Lasers in Cultural Heritage: The Non-Contact Intervention. *Springer Ser. Mater. Sci.* **2010**, *130*, 331–349.
73. Garbacz, H.; Fortuna, E.; Marczak, J.; Strzelec, M.; Rycyk, A.; Koss, A.; Mróz, J.; Zatorska, A.; Kurzydłowski, K. J. Laser Cleaning of Copper Roofing Sheets Subjected to Long-Lasting Environmental Corrosion. *Appl. Phys. A* **2010**, *100*, 693–701.
74. Garbacz, H.; Koss, A.; Marczak, J.; Mróz, J.; Onyszczuk, T.; Rycyk, A.; Sarzyński, A.; Skrzeczanowski, W.; Strzelec, M.; Zatorska, A. Optimized Laser Cleaning of Metal Artworks–Evaluation of Determinants. *Phys. Procedia* **2010**, *5*, 457–466.
75. Siano, S.; Agresti, J.; Cacciari, I.; Ciofini, D.; Mascalchi, M.; Osticioli, I.; Mencaglia, A. A. Laser Cleaning in Conservation of Stone, Metal, and Painted Artifacts: State of the Art and New Insights on the Use of the Nd: YAG Lasers. *Appl. Phys. A* **2012**, *106*, 419–446.
76. Sansonetti, A.; Colella, M.; Letardi, P.; Salvadori, B.; Striova, J. Laser Cleaning of a Nineteenth-Century Bronze Sculpture: In Situ Multi-Analytical Evaluation. *Stud. Conser.* **2015**, *60*, S28–S33.
77. Grigor'eva, I. A.; Parfenov, V. A.; Prokuratov, D. S.; Shakhmin, A. L. Laser Cleaning of Copper in Air and Nitrogen Atmospheres. *J. Opt. Technol.* **2017**, *84*, 1–4.
78. Di Francia, E.; Lahoz, R.; Neff, D.; Rico, V.; Nuns, N.; Angelini, E.; Grassini, S. Novel Procedure for Studying Laser-Surface Material Interactions During Scanning Laser Ablation Cleaning Processes on Cu-Based Alloys. *Appl. Surf. Sci.* **2021**, *544*, 148820.
79. Bertasa, M.; Korenberg, C. Successes and Challenges in Laser Cleaning Metal Artefacts: A Review. *J. Cult. Herit.* **2022**, *53*, 100–117.
80. Di Francia, E.; Lahoz, R.; Neff, D.; de Caro, T.; Angelini, E.; Grassini, S. Laser-Cleaning Effects Induced on Different Types of Bronze Archaeological Corrosion Products: Chemical-Physical Surface Characterisation. *Appl. Surf. Sci.* **2022**, *573*, 150884.
81. Shen, Y.; Zhang, G.; Zhou, X. Identification of an Unusual Pale Green Material on the Surface of an Ancient Chinese Bronze Vessel and Application of Laser Cleaning to its Removal. *Herit. Sci.* **2023**, *11*, 87.
82. Qian, R.; Wang, Q.; Niu, W.; Zhang, H.; Wei, C. Application of Laser Cleaning Technology on Metal Cultural Relics. *Surf. Sci. Technol.* **2023**, *1*, 26.
83. Hou, L.; Yin, F.; Wang, S.; Sun, J.; Yin, H. A Review of Thermal Effects and Substrate Damage Control in Laser Cleaning. *Opt Laser. Technol.* **2024**, *174*, 110613.
84. Bauer, A. Zur Frage der Erhaltung der öffentlichen Denkmäler. *Mittheilungen des k.k. Oesterrichischen Museums* **1882**, *17*, 1–15.
85. Bauer, A. Ueber Reinigung der Monumente. *Mittheilungen des k. k. Österreichischen Museums* **1885**, 1–16.
86. Baer, N. Conservation Notes: Maintenance of Outdoor Bronze Sculpture. *Int. J. Mus. Manag. Curatorsh.* **1988**, *7*, 71–75.
87. Sturman, S.; Unruh, J.; Spand, H. Maintenance of Outdoor Sculpture – an Annoted Bibliography. In *Maintenance of Outdoor Sculpture – An Annoted Bibliography*; National Institute for the Conservation of Cultural Property: Washington, D.C., 1996; p 70.

88. Degrigny, C. Survey of European Experiences on Cleaning Procedures. In *Monumenti in bronzo all'aperto: esperienze di conservazione a confronto*; Nardini Editore: Florence, 2004; pp 87–93.
89. Knotková, D.; Kreislová, K. Atmospheric Corrosion and Conservation of Copper And Bronze. *WIT Trans. State-of-the-art Sci. Eng.* **2007**, *28*.
90. Gigante, G. E.; Marabelli, M.; Cesareo, R.; Ridolfi, S. Strategy in the Preservation of Metal Monuments of Ancient and Modern Age: The Role of X Ray Techniques. In *XI Latin American Seminar of Analysis by X-Ray Techniques*; Rio de Janeiro, 2009; pp 1515–1565.
91. Conrad, W.; Wust, H.; Wiedemann, G. Freilegung von Grünpatina mit dem Laserstrahl. *Restauro* **1998**, *104*, 422–428.
92. Wolfe, J.; Grayburn, R. A Review of the Development and Testing of Incralac Lacquer. *J. Am. Inst. Conserv.* **2017**, *56*, 225–244.
93. Moffett, D. L. Wax Coatings on Ethnographic Metal Objects: Justifications for Allowing a Tradition to Wane. *J. Am. Inst. Conserv.* **1996**, *35*, 1–7.
94. Basso, E.; Pozzi, F.; Reiley, M. C. The Samuel F. B. Morse Statue in Central Park: Scientific Study and Laser Cleaning of a 19th-century American Outdoor Bronze Monument. *Herit. Sci.* **2020**, *8*, 81.
95. Letardi, P. Testing New Coatings for Outdoor Bronze Monuments: A Methodological Overview. *Coatings* **2021**, *11*, 131.
96. Mikić, D.; Otmačić Ćurković, H. Protection of Patinated Bronze with Long-Chain Phosphonic Acid/Organic Coating Combined System. *Materials* **2023**, *16*, 1660.
97. Eriksson, P.; Johansson, L. G.; Strandberg, H. Initial Stages of Copper Corrosion in Humid Air Containing SO_2 and NO_2. *J. Electrochem. Soc.* **1993**, *140*, 53–59.
98. Zakipour, S.; Tidblad, J.; Leygraf, C. Atmospheric Corrosion Effects of SO_2 and O_3 on Laboratory-Exposed Copper. *J. Electrochem. Soc.* **1995**, *142*, 757.
99. Tidblad, J.; Leygraf, C. Atmospheric Corrosion Effects of SO_2 and NO_2: A Comparison of Laboratory and Field-Exposed Copper. *J. Electrochem. Soc.* **1995**, *142*, 749.
100. Welter, J.-M. La couverture en cuivre en France: une promenade à travers les siècles. *Monumental* **2007**, 104–112.
101. Senn, M.; Degrigny, C. Shingle of a Roof. In *MiCorr*; Haute Ecole Arc Conservation-Restauration: Neuchâtel, 2022.